Toxicology
Research

ROYAL SOCIETY
OF CHEMISTRY

Effect of diselenide administration in thioacetamide-induced acute neurological and hepatic failure in mice

SCHOLARONE™
Manuscripts

Effect of diselenide administration in thioacetamide-induced acute neurological and hepatic failure in mice

Authors: Sílvio Terra Stefanello [a], Edovando José Flores da Rosa [a], Fernando Dobrachinski [a], Guilherme Pires Amaral [a], Nélson Rodrigues de Carvalho [a], Sônia Cristina Almeida da Luz [a], Caroline Raquel Bender [b], Ricardo S. Schwab [b], Luciano Dornelles [b], Félix Alexandre Antunes Soares [a*].

[a] Departamento de Bioquímica e Biologia Molecular, Centro de Ciências Naturais e Exatas, Universidade Federal de Santa Maria, Santa Maria, CEP 97105-900, Brazil

[b] Departamento de Química, Centro de Ciências Naturais e Exatas, Universidade Federal de Santa Maria, Santa Maria, CEP 97105-900, Brazil

[*]Corresponding author:

Félix Alexandre Antunes Soares-Departamento de Bioquímica e Biologia Molecular-CCNE Universidade Federal de Santa Maria-97105-900-Santa Maria-RS-Brazil.

Phone: +55-55-3220-9522. Fax: +55-55-3220-8978. E-mail: felix@ufsm.br

Abstract

Neurological disorders such as hepatic encephalopathy are a common complication of the severe acute hepatic failure that is associated with high short-term mortality rates. Therefore, the aim of this study was to investigate the effect of diphenyl diselenide (DPDS) and its analogues in protecting against thioacetamide (TAA)-induced acute neurological and hepatic failure in mice. The animals received a TAA dose of 200 mg/kg intraperitoneally, and then, 1 hour later, they received 15.6 mg/kg intraperitoneally of diselenides. Twenty three hours after diselenide administration, the animals were sacrificed, and blood, brain and liver samples were collected for analysis. The results showed that mice exposed to TAA presented oxidative stress characteristics, such as an increase in lipid peroxidation (LPO), enhanced glutathione peroxidase activity and decrease in the GSH/GSSH ratio in the brain and liver. In addition, the TAA group showed a decrease in cellular viability in both tissues. TAA treatments also generate reactive oxygen species and cause inhibition of glutathione-S-transferase in liver, which were associated with TAA exacerbated half-life in this tissue. In the histopathological analyses, we observed that TAA induced a large inflammation process that was confirmed according to the elevation of liver myeloperoxidase activity. Moreover, the treatment with diselenides reduced the oxidative stress significantly. Additionally, after the establishment of acute hepatic failure (AHF), DPDS was able to inhibit the inflammatory processes with a significant decrease in major hepatic damage effects than was presented after treatment with its analogues. Thus, our results showed that DPDS is a promising therapeutic option for the treatment of AHF and hepatic encephalopathy as mice returned to normal conditions after the damage.

Keywords: Diphenyl diselenide, thioacetamide-S-dioxide, new diselenides, liver damage, hepatic encephalopathy.

1. Introduction

Acute hepatic failure (AHF) is a severe liver injury characterized by serious complications of multiple organs and is also presented with high mortality rates when associated with the development of hepatic encephalopathy [1, 2].

Among various neurological and hepatic toxicity models, thioacetamide (TAA) is frequently used in experimental studies involving rodents to further evaluate the therapeutic potential of new drugs [3-5]. In addition, TAA is considered to be a strong hepatic toxin than can cause a severe disruption in liver metabolism and is associated with hepatocellular necrosis and hepatic encephalopathy [6, 7].

The hepatotoxicity induced by TAA occurs in a short time follow its administration due the formation of reactive metabolites, such as TAA sulfoxide and thioacetamide-S-dioxide ($TASO_2$) [7, 8]. $TASO_2$ is a strong reactive metabolite and consequently responsible for initiating the brain and liver necrosis process, depletion of endogenous antioxidant substrates, generation of reactive oxygen species (ROS) and lipid peroxidation [9-13]. Against TAA-induced injury, several antioxidants, such as organic selenium and phytochemical compounds, have been reported by protecting the brain and liver [14-19].

Classical organic selenium compounds, i.e. diphenyl diselenide (DPDS), have been recognized for their antioxidant, immunosuppressive and anti-inflammatory properties as well as neurological and hepatic-protective effects [20-23]. Studies involving DPDS also demonstrate its ability to reduce AHF caused by acetaminophen administration in mice [24-26].

Corresponding with the beneficial effects resulting from organic selenium compounds, new diselenides were produced through modifications in the DPDS molecule [27, 28]. Consequently, this study evaluates DPDS and its chemical analogues, which consist of an insertion of a methoxy (C1) or methyl (C2) group in the DPDS molecule (Figure 1). In addition, previous studies with these analogues have shown an expressive *in vitro* antioxidant effect [29].

Thus, the aim of the present experimental study was to evaluate whether the structural insertions of the new organic selenium compounds, methoxy (C1)

or methyl (C2) groups, or DPDS ameliorate the AHF induced by TAA when administered after the establishment of cellular damage. Hepatic failure was assessed by the measurement of serum alanine aminotransferase (ALT) and aspartate aminotransferase (AST) activities, myeloperoxidase and histopathological analysis. In addition, neurological and hepatic oxidative stress was estimated by measuring the brain and liver tissue levels of malondialdehyde (MDA), ROS production, GSH, GSSG, antioxidant enzymes (GST and GPx) and cellular viability.

2. Materials and methods

2.1. Chemicals

DPDS, TAA, thiobarbituric acid (TBA), malondialdehyde (MDA), methyltetrazolium bromide (MTT) and dimethyl sulfoxide (DMSO) were obtained from Sigma (St. Louis, MO). Tris–HCl, 2'7' dichlorofluorescein diacetate (H_2-DCFDA), sodium dodecyl sulfate (SDS), acetic acid, and ethanol were obtained from Merck (Rio de Janeiro, RJ, Brazil). All other chemicals were of analytical grade and were obtained from standard commercial suppliers.

2.2. Compounds

The DPDS analogues were prepared following according to the literature method previously described by Salman et al. in 2012 [30]. The products' purity was accessed by hydrogen and carbon nuclear magnetic resonance and gas chromatography. The compounds tested were 1,2-bis(2-methoxyphenyl)diselenide (C1) and 1,2-bis*p*-tolyldiselenide (C2). All of the compounds were dissolved in DMSO.

2.3. Animals

Male adult Swiss albino mice (25–35 g) from our own breeding colony were used. The animals were maintained on a 12-h light:12-h dark cycle at a room

temperature of 22 ± 2°C with free access to food and water. The animals were treated according to the standard guidelines of the Committee on Care and Use of Experimental Animal Resources. The protocol was approved by the Committee on the Ethics of Animal Experiments of the Federal University of Santa Maria, Brazil (Permit Number 101/2014).

2.4. Experimental treatments

The animals were divided into five groups with 5 mice each. The groups were classified as follows: groups I (saline – canola oil), II (TAA – canola oil), III (TAA – DPDS), IV (TAA – C1) and V (TAA – C2). Group I (control) received 0.9% saline and after 1 h received canola oil. Group II received TAA (200 mg/kg i.p.) and after 1 h received vehicle (canola oil 2.5 ml/kg i.p.) [9, 31]. Groups III, IV and V received TAA (200 mg/kg i.p.) dissolved in buffered saline, and after 1 h, they received the diselenides at 15.6 mg/kg i.p. (DPDS, C1 and C2, respectively) [26, 32]. The dose used for diselenides were considered safe due the DPDS LD_{50} calculated for i.p. administration in mice is 210 mmol/kg [33]. All mice were sacrificed 23 hours after receiving the diselenides or vehicle (scheme 1) by cervical dislocation. The blood was collected by cardiac puncture immediately after cervical dislocation. Serum was obtained by centrifuging the blood at 2,000 g for 10 min. The brains and livers were removed, weighed, dissected, and kept on ice until the time of the assay. The remaining portions of the liver were collected from the same anatomic area in all groups to perform the myeloperoxidase assay and the histopathological analyses. The other portion of the livers and the total brains were homogenized in 10 mM Tris–HCl, pH 7.4 (1/10, w/v) and centrifuged at 2000 g for 10 min, and the low-speed supernatants (S1) were separated and used for experiments. The compounds control group presented similar effect than saline (data not shown).

2.5. Measurement of body and relative tissue weights

The body weight was measured minutes before the sacrifice. After the cervical dislocation, the mouse brains and livers were weighted. Relative weights were calculated according to the equation below.

$$\text{Relative organ weight} = \frac{\text{Absolute Organ Weight}}{\text{Body Weight at Sacrifice}} \times 100\%$$

2.6. Measurement of Serum ALT and AST Level

Serum activities of alanine aminotransferase (ALT) and aspartate aminotransferase (AST) were estimated by spectrophotometry using commercially available kits (Labtest, Diagnostica S.A., Minas Gerais, Brazil).

2.7. MTT Reduction Levels

MTT reduction levels were determined as an index of dehydrogenase enzymatic functions, which are involved in cellular viability [34]. Aliquots of liver and brain S1 (200 µL) were added to a medium containing 0.5 mg/mL of MTT and were incubated in the dark for 60 min at 37°C. The MTT reduction reaction was quenched with the addition of 1 mL of DMSO. Formazan levels were measured spectrophotometrically at 570 nm, and the results were corrected by the protein content [35].

2.8. Thiobarbituric Acid–Reactive Substances Levels

The end products of lipid peroxidation were determined in tissue samples as previously described Ohkawa et al. 1979 [36]. Aliquots (200 µL) of brain and liver supernatants were mixed with 500 µL of TBA (0.6%), 200 µL of SDS (8.1%), and 500 µl of acetic acid (pH 3.4). The color reaction was developed by incubating the tubes in boiling water for 60 min. TBARS levels were measured at 532 nm using a standard curve of MDA, and the results were reported as nmol MDA/mg protein.

2.9. Measurement of Intracellular Reactive Oxygen Species Production

2'-7'-Dichlorofluorescein (DCF) levels was utilized to measure the intracellular formation of ROS by the cellular components [37]. Aliquots (20 µl) of brain and liver supernatants were added to a medium containing Tris–HCl buffer (10 mM; pH 7.4) and 2'-7'-dichlorofluorescein diacetate DCFH-DA (1 mM). After DCFH-DA addition, the medium was incubated in the dark for 60 min until the fluorescence was measured (excitation at 488 nm and emission at 525 nm, and both slit widths used were at 1.5 nm). DCF levels were determined using a standard curve of DCF, and the results were corrected by the protein content.

2.10. Myeloperoxidase (MPO) Activity

The MPO enzymatic activity was determined in the liver according to the method proposed previously Grisham et al. 1986 with some modifications [38]. Briefly, a sample of liver supernatant (20 µL) was added to a medium containing potassium phosphate buffer (50 mM; pH 6.0), hexadecyltrimethylammonium bromide (0.5%), and N, N, N', N'-tetramethylbenzidine (1.5 mM). The kinetic analysis of MPO was started after H_2O_2 (0.01%) addition, and the color reaction was determined at 655 nm at 37°C.

2.11. Measurement of reduced (GSH) and oxidized (GSSG) glutathione

For the measurement of GSH and GSSG levels, we used a method previously described Hissin and Hilf 1976 [39]. In brief, 250 mg of brain and liver were homogenized in 3.75 mL of phosphate EDTA buffer (pH 8) plus 1 mL of H_3PO_4 (25%). Homogenates were centrifuged at 4°C at 130,000 g for 30 min, and the supernatants (S2) were separated in two different aliquots of 500 µL each for measurement of GSH and GSSG. For GSH determination, 100 µL of the supernatant (S2) was diluted in 1.8 mL of phosphate buffer and 100 µL of O-phthalaldehyde (OPT) (1 µg/µL). The mixtures were incubated at room temperature for 15 min and their fluorescent signals were recorded in the RF-5301 PC Shimadzu spectrofluorometer (Kyoto, Japan) at 420 nm for emission and 350 nm for excitation wavelengths. For measurement of GSSG levels, 250 µL of the supernatant (S2) was incubated at room temperature with 100 µL of N-ethylmaleimide (NEM) (0.04 M) for 30 min at room temperature, and after

that, 140 µL of the mixture was added to 1.760 mL of NaOH (0.1 N) buffer, followed with the addition of 100 µL of OPT and then incubated for 15 min using the procedure outlined above for GSH assay.

2.12. Measurement of Glutathione-S-transferase (GST)

Glutathione-S-transferase (GST) activity was determined spectrophotometrically [40]. GST activity was quantified in brain and liver homogenate supernatant (S1) in a reaction mixture containing 1 mM 1-chloro-2,4-dinitrobenzene (CDNB) and 1 mM glutathione as substrates in 0.1 M sodium phosphate buffer, pH 6.5, at 37°C. Enzymatic activity was calculated by the change in the absorbance value from the slope of the initial linear portion of the absorbance time curve at 340 nm for 5 min. Enzymatic activity was determined using the molar extinction coefficient 9.6 mM-1 cm-1 and was expressed as nmol CDNB/min/mg protein.

2.13. Measurement of Glutathione Peroxidase (GPx)

Glutathione peroxidase (GPx) activity was determined spectrophotometrically at 340 nm by NADPH consumption for 2 min at 30ºC [41]. The brain and liver homogenate supernatant (S1) was added to medium containing 0.1 M phosphate buffer (0.1 M KH_2PO_4 and 5 mM EDTA, pH 7.0), 1 mM GSH, 0.15 mM NADPH, 0.1 U/mL glutathione reductase and 1 mM sodium azide. Thus, the reaction was initiated by adding the H_2O_2 to a final concentration of 0.4 mM. The GPx activity was determined using the molar extinction coefficient 6220 M^{-1} cm^{-1} and was expressed as nmol/min/mg protein.

2.14. Histopathological observation

Liver tissues were fixed in 10% formalin and then embedded in paraffin. Tissue sections (4-µm thickness, n = 5 mice per group) were stained with hematoxylin and eosin (H&E) and observed under a light microscope by an expert in histology who was blinded to the treatments.

2.15. Protein quantification

The protein concentration was estimated by the Bradford method using bovine serum albumin as the standard [42].

2.16. Statistical analysis

All data are expressed as means ± S.E.M for each experimental group. Determination of statistical significance was performed by a two-way analysis of variance (ANOVA), followed by Bonferroni post-test when appropriate. Differences between groups were considered to be significant when $p<0.05$.

3. Results

3.1. Index

The administration of a toxic dose of TAA caused a significant increase in the brain and liver weight, indicating edema formation in both tissues (Figure 2). The treatment with diselenides restored the brain and liver weights to control levels, indicating the hepatic protective effect of organic selenium compounds toward TAA toxicity.

3.2. Biochemical Assay

The serum concentrations of both AST (A) and ALT (B), used as markers of liver damage, were significantly greater in the TAA group (Figure 3). The animals treated with DPDS exhibited AST and ALT activities similar to those of the control group and significantly lower activities of both AST and ALT when compared with the TAA group, indicating a reduction in tissue damage. However, the compounds C1 and C2 exhibited AST and ALT activities similar to the TAA group.

3.3. Mitochondrial Dehydrogenases Activity (MTT)

The MTT reduction assay showed that TAA caused a significant decrease in the brain (A) and liver (B) cell viability compared with the control (Figure 4). In addition, we observed that treatment with diselenides was able to significantly minimize the toxic effects of TAA in both tissues, demonstrating that the treatment was able to protect against the damage caused by TAA.

3.4. Thiobarbituric Acid Reactive Substance Levels

The administration of TAA caused a significant increase in lipid peroxidation, as determined by the increase in MDA levels in the brain (A) and liver (B), indicating damage caused by oxidative stress (Figure 5). Mice that received treatments with diselenides exhibited a significant reduction of TAA-induced MDA formation, indicating a marked reduction in oxidative stress in both tissues.

3.5. Quantification ROS Production

Mice that received treatment with both TAA and diselenides maintained the same intracellular levels of ROS in the brain as the control group (Figure 6A). However, in the liver (Figure 6B), the TAA administration caused a significant increase in the ROS production compared with the control group. DPDS, C1 and C2 significantly reduced the DFC formation caused by TAA in the liver.

3.6. Myeloperoxidase Activity

Treatment with TAA initiated an inflammatory process, as evidenced by the significant increase in MPO activity compared with the control group (Figure 7). The group treated with DPDS and C1 presented a significant reduction in MPO activity compared with the TAA group. No difference in the inflammatory processes was found between the group treated with C2 and the group treated only with TAA.

3.7. GSH and GSSG levels

All groups presented similar GSH levels in the brain (Figure 8A). However, TAA induced a significant increase in the brain GSSG levels, and the diselenides were able to significantly reduce this increase to control levels (Figure 8B). Figure 8C and 8D demonstrate that the administration of TAA markedly decreased the liver GSH and GSSG levels compared with the control group. Treatment with diselenides prevented the TAA-induced depletion of liver GSH observed in the TAA group and raised the GSSG levels, indicating an improvement in the antioxidant defense system.

The administration of TAA caused a significant reduction in brain and liver GSH/GSSG ratio (Figure 8E and 8F) compared with the control group, and the treatment with diselenides were different than TAA group.

3.8. Effects of TAA on antioxidant enzyme activities

Treatments with TAA and diselenides elevated the brain GST levels significantly when compared with the control group. However, C1 exhibited the brain GST levels significantly different from the TAA (Figure 9A). In addition, the TAA and diselenides caused a significant inhibition of the liver GST activity when compared with the control group (Figure 9B). Figure 9C and 9D illustrates that the administration of TAA and diselenides significantly increased the brain and liver GPx levels in comparison to the control group.

3.9. Histopathology

A histopathological assessment of the liver was performed for all groups. The livers of mice in the control group (Figure 10 A1-2) showed normal, well-defined histological structures with the absence of hepatocellular injury, necrosis and vascular congestion. The histopathological analysis of the livers from mice in the TAA group (Figure 10 B1-2) revealed signs of toxicity with severe morphological changes and the presence of sinusoidal congestion (SC), vacuolar degeneration (VD), necrotic hepatocytes, macrophage infiltration (MI) and nuclear pyknosis (NP), with spillage of red blood cells in between hepatocytes. In contrast, the animals treated with DPDS (Figure 10 C1-2)

exhibited a reduction in the TAA-induced changes, with less microvesicular steatosis, characterized by the presence of small fatty vesicles filling the cytoplasm of the hepatocyte. However, treatment with C1 and C2 presented a necrotic area with a wide distribution in hepatic parenchyma as well as a SC, VD, MI and NP (Figure 10 D1-2 and E1-2).

4. Discussion

The present study aimed to investigate and clarify the protective properties of diselenide compounds over TAA-induced AHF after the establishment of the damage. Recent studies have shown that organic selenium compounds presented promising hepatic and neurological pharmacological properties [25, 26, 43].

In this way, experimental models involving a single dose of TAA (200 mg/mL) were able to induce liver injury, which can be demonstrated by high AST and ALT enzyme activities [31]. According to our findings, TAA led to a 2.12-fold higher increase in the AST activity and a 9.52-fold higher increase in ALT activity compared to the control group, providing evidence to the TAA-induced acute hepatotoxicity (Fig. 3). However, the administration of DPDS maintained AST and ALT activities similar to the control group, demonstrating that the classical selenium compound was able to protect the TAA-induced AHF. The compounds C1 and C2 presented AST and ALT activities comparable to the TAA group, indicating that the molecular methoxy and methyl insertions on the DPDS structure did not enhance their protective effect.

Additionally, liver is considered to be the responsible organ for toxicity regulation by housing the metabolic functions that can serve to detoxify several toxins [44]. However, these metabolic functions render the hepatic cells vulnerable to a variety of disorders [44, 45]. In this context, liver diseases can develop dysfunctions in other tissues; i.e. causing the release of activated immune cells and trigger the reactive oxygen species-mediated cell killing process [25, 46]. Previous studies have reported that a single dose of TAA at 40 mg/kg can cause cell death, apoptosis and necrosis in rats with a considerable increase in organ weight, indicating that AHF can also promote tissue congestion [47, 48]. Similarly, the TAA treated group demonstrated a significant

increase in brain and liver weight, however such increasing was not observed in the mice exposed to the diselenide compounds (Fig. 2). We also showed in the MTT assay that a single administration of TAA diminished the cellular viability in both tissues and that diselenides were able to protect the TAA cellular disruption (Fig. 4). Thus, these findings showed that the diselenides could preserve the anatomic characteristics of the brain and liver and also the cellular viability in both tissues after the damage was established by TAA.

Furthermore, the excessive formation of the metabolite $TASO_2$ as the primary mechanism which promotes AHF, and it was closely linked with oxidative stress generation, i.e. lipid peroxidation, and ROS production. [7, 10, 49]. Thus, we showed in this study that TAA induces an increase in lipid peroxidation in both brain and liver (Fig. 5A and 5B). We also verified that the treatment with diselenides exerted a significant decrease on MDA levels in both tissues, demonstrating the ability of the organic selenium compounds to promote their antioxidant effects after the damage had already been provoked. Additionally, previous *in vitro* studies had shown that diselenides were promising molecules to reduce the LPO in brain and liver, which has been strongly attributed to the selenol group formation [29, 50].

Moreover, TAA increased the ROS production in the liver, and treatment with diselenides were able to maintain such levels similar to the control group (Fig. 6B). Conversely, our results presented that TAA administration did not affect ROS production in the brain (Fig. 6A), which could be justified by a compensatory mechanism produced by GST and GPx (Fig. 9A and 9C) against oxidative stress conditions reported in previous studies [51, 52]. Accordingly, it has been known that high levels of TAA remain longer in the liver than in the brain, which can explain the differences founded in the oxidative parameters over those tissues [7, 10]. Thus, our results showed that TAA caused significant inhibition in liver GST, differently to diselenides (Fig. 9B). Furthermore, TAA invoke an elevation in the liver GPx activity while diselenides kept different to those of the control group (Fig. 9D).

Additionally, liver diseases seriously impact in clinical medicine because of the high mortality rates of patients associated with the severe damaged caused by AHF [53]. As such, previous studies have already demonstrated the important role of AHF in generating multiple organ failure through endogenous

antioxidant defense depletion [25, 54]. In addition, the endogenous antioxidant system mainly consists of GSH and several antioxidant enzymes such as GPx and TrxR [50, 55-57]. Therefore, the redox mechanism composed by GSH is able to convert the harmful agents into metabolites which are easier eliminated; and generally resulting in a decrease over GSH stores [24, 39, 58]. Corroborating to this hypothesis, we observed that the treatment with TAA resulted in a significant reduction in liver GSH levels as a possible mechanism of the $TASO_2$ metabolite conjugation (Fig. 8C). Similarly, we also showed that treatment with both TAA and diselenides did not change the brain GSH levels (Fig. 8A). However, TAA treatment produced a significant decrease in the brain and liver GSH/GSSG ratio (Fig. 8E and 8F), which could be contributing to the imbalance of endogenous antioxidant defenses. Diselenides were able to maintain the brain and liver GSH/GSSG ratio similar that control group.

Other mechanisms involved in the disorders caused by TAA administration are related with the release of proinflammatory mediators [14]. Moreover, neutrophil infiltration is a key factor in initiating TAA-induced AHF, and the increase in MPO activity can be associated with ROS formation and other inflammatory processes [26, 59]. Therefore, our results confirmed that TAA induced an elevation in MPO activity, indicating the progression of inflammatory processes in the liver (Fig. 7). Similarly, previous studies have reported that pre-treatment with DPDS exhibited an anti-inflammatory effect when acute hepatic damage was induced with either 2-nitropropane or paraquat in rats [60, 61]. We also found that post-treatment with DPDS was able to significantly decrease the MPO activity, revealing a reduction in the liver inflammatory process. In addition, the analogues of DPDS presented a decrease in MPO activity, but only the C1 showed a significant effect compared with the TAA group. Therefore, our results indicated that treatment with diselenides promoted an important reversion of the inflammatory processes caused by TAA. Moreover, the histopathological analysis showed that TAA caused severe damage in the liver with a presence of hemorrhagic massive necrosis and severe steatosis (Fig. 10 B1-2). Further, we could verify the presence of infiltrated leukocytes in the TAA treated group. However, treatment with DPDS (Fig. 10 C1-2) led to the retention of liver characteristics similar to the control group (Fig. 10 A1-2) without showing necrotic and hemorrhagic

zones. C1 and C2 did not cause any improvement in liver conditions because some areas were still presenting steatosis, hemorrhagic and necrotic characteristics (Fig. 10 D1-2 and E1-2).

Therefore, we observed that DPDS administration one hour after TAA administration was able to re-establish the normal biochemical and histopathological parameters in the brain and liver. However, the analogues C1 and C2, although they were able to present some protective effects compared with the TAA group and similar than found in previous *in vitro* studies, did not revert the AHF [29].

In conclusion, DPDS presented a higher reversion effect than its analogues and could be showed again as a promising therapeutic option for the treatment of AHF, such as hepatic encephalopathy.

5. Conflicts of interest

The authors declare that there are no conflicts of interest.

Acknowledgments

References

1. Demirel, U., et al., *Allopurinol ameliorates thioacetamide-induced acute liver failure by regulating cellular redox-sensitive transcription factors in rats.* Inflammation, 2012. **35**(4): p. 1549-57.

2. Tunon, M.J., et al., *An overview of animal models for investigating the pathogenesis and therapeutic strategies in acute hepatic failure.* World J Gastroenterol, 2009. **15**(25): p. 3086-98.

3. Yogalakshmi, B., P. Viswanathan, and C.V. Anuradha, *Investigation of antioxidant, anti-inflammatory and DNA-protective properties of eugenol in thioacetamide-induced liver injury in rats.* Toxicology, 2010. **268**(3): p. 204-12.

4. Shapiro, H., et al., *Curcumin ameliorates acute thioacetamide-induced hepatotoxicity.* Journal of Gastroenterology and Hepatology, 2006. **21**(2): p. 358-366.

5. Chadipiralla, K., et al., *Thioacetamide-induced fulminant hepatic failure induces cerebral mitochondrial dysfunction by altering the electron transport chain complexes.* Neurochem Res, 2012. **37**(1): p. 59-68.

6. Avraham, Y., et al., *Endocannabinoids affect neurological and cognitive function in thioacetamide-induced hepatic encephalopathy in mice.* Neurobiol Dis, 2006. **21**(1): p. 237-45.

7. Chilakapati, J., et al., *Toxicokinetics and toxicity of thioacetamide sulfoxide: a metabolite of thioacetamide.* Toxicology, 2007. **230**(2-3): p. 105-16.

8. Chieli, E. and G. Malvaldi, *Role of the microsomal fad-containing monooxygenase in the liver toxicity of thioacetamide S-oxide.* Toxicology, 1984. **31**(1): p. 41-52.

9. Porter, W.R. and R.A. Neal, *Metabolism of thioacetamide and thioacetamide S-oxide by rat liver microsomes.* Drug Metabolism and Disposition, 1978. **6**(4): p. 379-388.

10. Chilakapati, J., et al., *Saturation toxicokinetics of thioacetamide: role in initiation of liver injury.* Drug Metab Dispos, 2005. **33**(12): p. 1877-85.

11. Ingawale, D.K., S.K. Mandlik, and S.R. Naik, *Models of hepatotoxicity and the underlying cellular, biochemical and immunological mechanism(s): a critical discussion.* Environ Toxicol Pharmacol, 2014. **37**(1): p. 118-33.

12. Abdel Salam, O.M., et al., *The effect of antidepressant drugs on thioacetamide-induced oxidative stress.* Eur Rev Med Pharmacol Sci, 2013. **17**(6): p. 735-44.

13. Koen, Y.M., et al., *Protein targets of thioacetamide metabolites in rat hepatocytes.* Chem Res Toxicol, 2013. **26**(4): p. 564-74.

14. de David, C., et al., *Role of quercetin in preventing thioacetamide-induced liver injury in rats.* Toxicol Pathol, 2011. **39**(6): p. 949-57.

15. Hsieh, C.-C., H.-L. Fang, and W.-C. Lina, *Inhibitory effect of Solanum nigrum on thioacetamide-induced liver fibrosis in mice.* Journal of Ethnopharmacology, 2008. **119**(1): p. 117-121.

16. Aydın, A.F., et al., *Effect of carnosine against thioacetamide-induced liver cirrhosis in rat.* Peptides, 2010. **31**(1): p. 67-71.

17.   Al-Bader, A., et al., *Selenium and liver cirrhosis.* Mol Cell Biochem, 1998. **185**(1-2): p. 1-6.

18.   Al-Bader, A.A., et al., *Effect of dietary selenium, zinc and allopurinol supplements on plasma and tissue manganese levels in rats with thioacetamide [correction of thiocetamide]-induced liver cirrhosis.* Mol Cell Biochem, 1997. **173**(1-2): p. 121-5.

19.   Sathyasaikumar, K.V., et al., *Co-administration of C-Phycocyanin ameliorates thioacetamide-induced hepatic encephalopathy in Wistar rats.* Journal of the Neurological Sciences, 2007. **252**(1): p. 67-75.

20.   de Freitas, A.S. and J.B. Rocha, *Diphenyl diselenide and analogs are substrates of cerebral rat thioredoxin reductase: a pathway for their neuroprotective effects.* Neurosci Lett, 2011. **503**(1): p. 1-5.

21.   Borges, L.P., et al., *Protective effect of diphenyl diselenide on acute liver damage induced by 2-nitropropane in rats.* Toxicology, 2005. **210**(1): p. 1-8.

22.   Nogueira, C.W., et al., *Anti-inflammatory and antinociceptive activity of diphenyl diselenide.* Inflamm Res, 2003. **52**(2): p. 56-63.

23.   Nogueira, C.W., et al., *Investigations into the potential neurotoxicity induced by diselenides in mice and rats.* Toxicology, 2003. **183**(1-3): p. 29-37.

24.   Carvalho, N.R., et al., *New therapeutic approach: diphenyl diselenide reduces mitochondrial dysfunction in acetaminophen-induced acute liver failure.* PLoS One, 2013. **8**(12): p. e81961.

25.   da Silva, M.H., et al., *Acute brain damage induced by acetaminophen in mice: effect of diphenyl diselenide on oxidative stress and mitochondrial dysfunction.* Neurotoxicity Research, 2012. **21**(3): p. 334-44.

26.   da Rosa, E.J., et al., *Reduction of acute hepatic damage induced by acetaminophen after treatment with diphenyl diselenide in mice.* Toxicol Pathol, 2012. **40**(4): p. 605-13.

27.   Paulmier, C., *Selenium reagents and intermediates in organic synthesis.* 1986: Pergamon.

28.   Mugesh, G., W.-W. du Mont, and H. Sies, *Chemistry of Biologically Important Synthetic Organoselenium Compounds.* Chemical Reviews, 2001. **101**(7): p. 2125-2180.

29.   Stefanello, S.T., et al., *Evaluation of in vitro antioxidant effect of new mono and diselenides.* Toxicology in Vitro, 2013. **27**(5): p. 1433-1439.

30.   Salman, S.M., et al., *CuO nano particles and [bmim]BF4: an application towards the synthesis of chiral [small beta]-seleno amino derivatives via ring opening reaction of aziridines with diorganyl diselenides.* RSC Advances, 2012. **2**(22): p. 8478-8482.

31.   Zhang, J., H. Wang, and H. Yu, *Thioacetamide-induced cirrhosis in selenium-adequate mice displays rapid and persistent abnormity of hepatic selenoenzymes which are mute to selenium supplementation.* Toxicol Appl Pharmacol, 2007. **224**(1): p. 81-8.

32.   Rosa, R.M., et al., *DNA damage in tissues and organs of mice treated with diphenyl diselenide.* Mutation Research/Genetic Toxicology and Environmental Mutagenesis, 2007. **633**(1): p. 35-45.

33.   Nogueira, C.W., et al., *Investigations into the potential neurotoxicity induced by diselenides in mice and rats.* Toxicology, 2003. **183**(1–3): p. 29-37.

34. Bernas, T. and J. Dobrucki, *Mitochondrial and nonmitochondrial reduction of MTT: interaction of MTT with TMRE, JC-1, and NAO mitochondrial fluorescent probes.* Cytometry, 2002. **47**(4): p. 236-42.

35. Mosmann, T., *Rapid colorimetric assay for cellular growth and survival: application to proliferation and cytotoxicity assays.* J Immunol Methods, 1983. **65**(1-2): p. 55-63.

36. Ohkawa, H., N. Ohishi, and K. Yagi, *Assay for lipid peroxides in animal tissues by thiobarbituric acid reaction.* Anal Biochem, 1979. **95**(2): p. 351-8.

37. Myhre, O., et al., *Evaluation of the probes 2',7'-dichlorofluorescin diacetate, luminol, and lucigenin as indicators of reactive species formation.* Biochemical Pharmacology, 2003. **65**(10): p. 1575-1582.

38. Grisham, M.B., L.A. Hernandez, and D.N. Granger, *Xanthine oxidase and neutrophil infiltration in intestinal ischemia.* Am J Physiol, 1986. **251**(4 Pt 1): p. G567-74.

39. Hissin, P.J. and R. Hilf, *A fluorometric method for determination of oxidized and reduced glutathione in tissues.* Analytical Biochemistry, 1976. **74**(1): p. 214-226.

40. Habig, W.H., M.J. Pabst, and W.B. Jakoby, *Glutathione S-Transferases: THE FIRST ENZYMATIC STEP IN MERCAPTURIC ACID FORMATION.* Journal of Biological Chemistry, 1974. **249**(22): p. 7130-7139.

41. Flohe, L. and W.A. Gunzler, *Assays of glutathione peroxidase.* Methods Enzymol, 1984. **105**: p. 114-21.

42. Bradford, M.M., *A rapid and sensitive method for the quantitation of microgram quantities of protein utilizing the principle of protein-dye binding.* Anal Biochem, 1976. **72**: p. 248-54.

43. Dobrachinski, F., et al., *Neuroprotective Effect of Diphenyl Diselenide in a Experimental Stroke Model: Maintenance of Redox System in Mitochondria of Brain Regions.* Neurotoxicity Research, 2014: p. 1-14.

44. Gill, R.Q. and R.K. Sterling, *Acute liver failure.* J Clin Gastroenterol, 2001. **33**(3): p. 191-8.

45. Begriche, K., et al., *Drug-induced toxicity on mitochondria and lipid metabolism: Mechanistic diversity and deleterious consequences for the liver.* Journal of Hepatology, 2011. **54**(4): p. 773-794.

46. Wang, M.E., et al., *Curcumin protects against thioacetamide-induced hepatic fibrosis by attenuating the inflammatory response and inducing apoptosis of damaged hepatocytes.* J Nutr Biochem, 2012. **23**(10): p. 1352-66.

47. Kadir, F.A., et al., *Hepatoprotective Role of Ethanolic Extract of Vitex negundo in Thioacetamide-Induced Liver Fibrosis in Male Rats.* Evid Based Complement Alternat Med, 2013. **2013**: p. 739850.

48. Ledda-Columbano, G.M., et al., *Induction of two different modes of cell death, apoptosis and necrosis, in rat liver after a single dose of thioacetamide.* Am J Pathol, 1991. **139**(5): p. 1099-109.

49. Low, T.Y., et al., *A proteomic analysis of thioacetamide-induced hepatotoxicity and cirrhosis in rat livers.* Proteomics, 2004. **4**(12): p. 3960-3974.

50. Prestes, A.S., et al., *Antioxidant activity of beta-selenoamines and their capacity to mimic different enzymes.* Mol Cell Biochem, 2012. **365**(1-2): p. 85-92.

51. Brigelius-Flohé, R., *Tissue-specific functions of individual glutathione peroxidases.* Free Radical Biology and Medicine, 1999. **27**(9–10): p. 951-965.

52. Armstrong, R.N., *Structure, Catalytic Mechanism, and Evolution of the Glutathione Transferases.* Chemical Research in Toxicology, 1997. **10**(1): p. 2-18.

53. Williams, R., S.W. Schalm, and J.G. O'Grady, *Acute liver failure: redefining the syndromes.* The Lancet, 1993. **342**(8866): p. 273-275.

54. Rama Rao, K.V., et al., *Aquaporin-4 deletion in mice reduces encephalopathy and brain edema in experimental acute liver failure.* Neurobiol Dis, 2014. **63**: p. 222-8.

55. Nogueira, C.W., G. Zeni, and J.B. Rocha, *Organoselenium and organotellurium compounds: toxicology and pharmacology.* Chem Rev, 2004. **104**(12): p. 6255-85.

56. Nogueira, C.W. and J.B.T. Rocha, *Diphenyl diselenide a janus-faced molecule.* Journal of the Brazilian Chemical Society, 2010. **21**: p. 2055-2071.

57. Nogueira, C.W. and J.B. Rocha, *Toxicology and pharmacology of selenium: emphasis on synthetic organoselenium compounds.* Arch Toxicol, 2011. **85**(11): p. 1313-59.

58. Ketterer, B., B. Coles, and D.J. Meyer, *The role of glutathione in detoxication.* Environ Health Perspect, 1983. **49**: p. 59-69.

59. Hsu, D.-Z., et al., *Role of flavin-containing-monooxygenase-dependent neutrophil activation in thioacetamide-induced hepatic inflammation in rats.* Toxicology, 2012. **298**(1–3): p. 52-58.

60. Borges, L.P., et al., *Protective effect of diphenyl diselenide on acute liver damage induced by 2-nitropropane in rats.* Toxicology, 2005. **210**(1): p. 1-8.

61. Costa, M.D., et al., *Diphenyl diselenide prevents hepatic alterations induced by paraquat in rats.* Environ Toxicol Pharmacol, 2013. **36**(3): p. 750-8.

Figures and legends

Fig. 1: Chemical structure of the compounds

Scheme 1: Demonstrative figure of experimental protocol

Fig. 2: Effect of TAA administration and treatment with diselenides in the brain index (A) and liver index (B). Data are shown as the means ± S.E.M, n=5, and the significance was assessed by two-way analysis of variance (ANOVA) followed by Bonferroni post-test. * Represents $p < 0.05$ if compared with the control group. # Indicates $p < 0.05$ compared with the TAA group.

Fig. 3: Effect of TAA administration and treatment with diselenides in AST (A) and ALT (B) activities. Data are shown as the means ± S.E.M, n=5, and the significance was assessed by two-way analysis of variance (ANOVA) followed by Bonferroni post-test. * Represents $p < 0.05$ if compared with the control group. # Indicates $p < 0.05$ compared with the TAA group.

Fig. 4: Effect of TAA administration and treatment with diselenides on cellular viability in the brain (A) and liver (B). Data are shown as the means ± S.E.M, n=5, and the significance was assessed by two-way analysis of variance (ANOVA) followed by Bonferroni post-test. * Represents $p < 0.05$ if compared with the control group. # Indicates $p < 0.05$ compared with the TAA group.

Fig. 5: Effect of TAA administration and treatment with diselenides in TBARS production in the brain (A) and liver (B). Data are shown as the means ± S.E.M, n=5, and the significance was assessed by two-way analysis of variance (ANOVA) followed by Bonferroni post-test. * Represents $p < 0.05$ if compared with the control group. # Indicates $p < 0.05$ compared with the TAA group.

Fig. 6: Effect of TAA administration and treatment with diselenides in ROS production in the brain (A) and liver (B). Data are shown as the means ± S.E.M, n=5, and the significance was assessed by two-way analysis of variance (ANOVA) followed by Bonferroni post-test. * Represents $p < 0.05$ if compared with the control group. # Indicates $p < 0.05$ compared with the TAA group.

Fig. 7: Effect of TAA administration and treatment with diselenides in liver myeloperoxidase levels. Data are shown as the means ± S.E.M, n=5, and the significance was assessed by two-way analysis of variance (ANOVA) followed by Bonferroni post-test. * Represents $p < 0.05$ if compared with the control group. # Indicates $p < 0.05$ compared with the TAA group.

Fig. 8: Effect of TAA administration and treatment with diselenides in GSH and GSSG levels, illustrating the brain GSH levels, GSSG levels and the ratio (A,B and E) and the liver GSH levels, GSSG levels and the ratio (C,D and F). Data

are shown as the means ± S.E.M, n=5, and the significance was assessed by two-way analysis of variance (ANOVA) followed by Bonferroni post-test. * Represents $p < 0.05$ if compared with the control group. # Indicates $p < 0.05$ compared with the TAA group.

Fig. 9: Effect of TAA administration and treatment with diselenides in the brain GST (A) and GPx levels (C) and in the liver GST (B) and GPx levels (D). Data are shown as the means ± S.E.M, n=5, and the significance was assessed by two-way analysis of variance (ANOVA) followed by Bonferroni post-test. * Represents $p < 0.05$ if compared with the control group. # Indicates $p < 0.05$ compared with the TAA group.

Fig. 10: Figures A1–E1 (H&E stain 10X) and Figures A2–E2 (H&E stain 40X). Black arrow represents the zonal necrosis, and the blue arrow represents the micro and macrovesicular steatosis. Livers from a control mouse (A) showing no changes in hepatocytes around the centrilobular (CV) area. The TAA group (B) with histopathological changes in the liver showed nuclear pyknosis (NP), vacuolar degeneration (VD), sinusoidal congestion (SC), necrotic hepatocytes (circles) and disorganization of hepatic laminae. The sections from livers treated with DPDS (C) showed normal histological appearance of the liver with hepatocytes adjacent to CV with absence of necrosis and vascular congestion. The sections from liver treated with C1 (D) and C2 (E) showed NP, SC, VD, steatosis and necrotic areas.
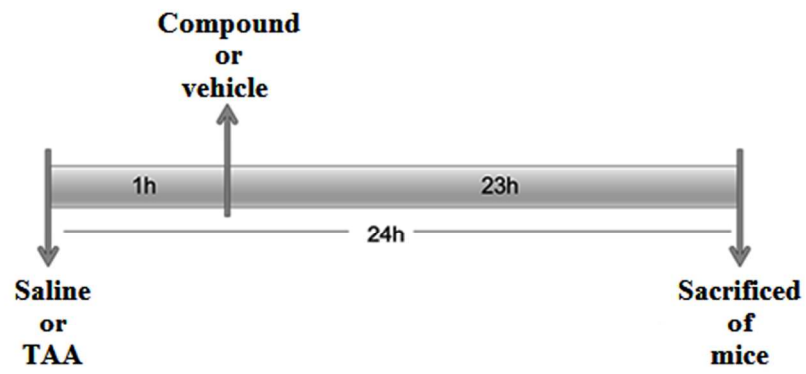
Scheme 1
59x27mm (600 x 600 DPI)
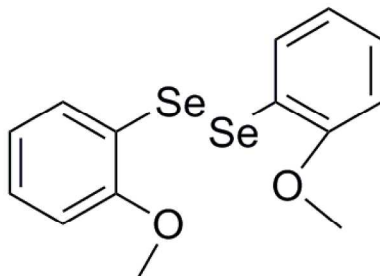
1,2-bis(2-methoxyphenyl)diselenide
C1
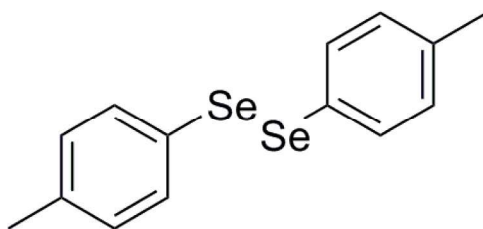
1,2-bis*p*-tolyldiselenide
C2
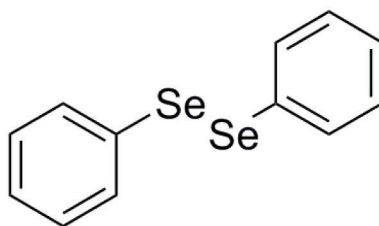
diphenyl diselenide
DPDS

Fig 1
99x133mm (600 x 600 DPI)

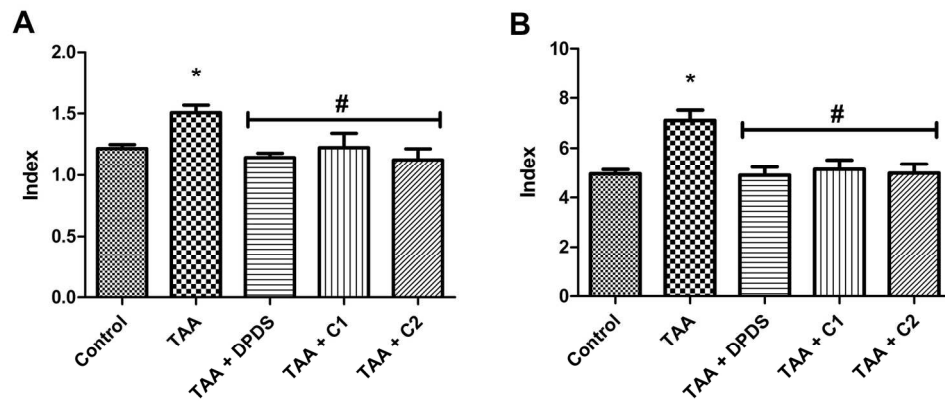Fig 2
82x36mm (600 x 600 DPI)
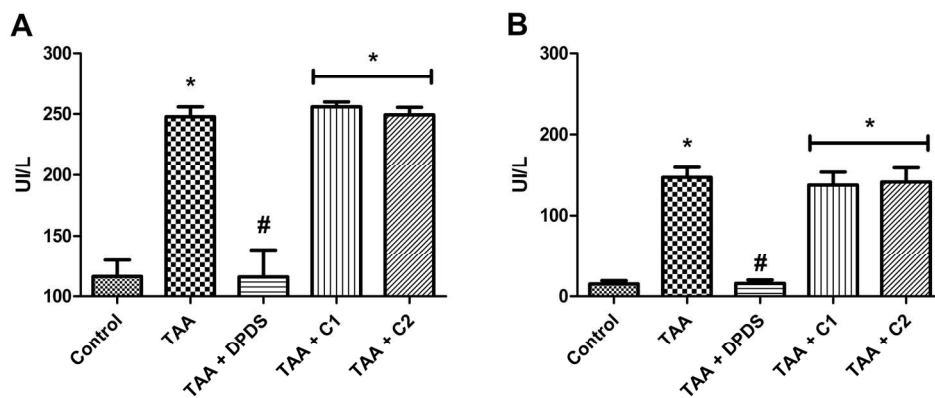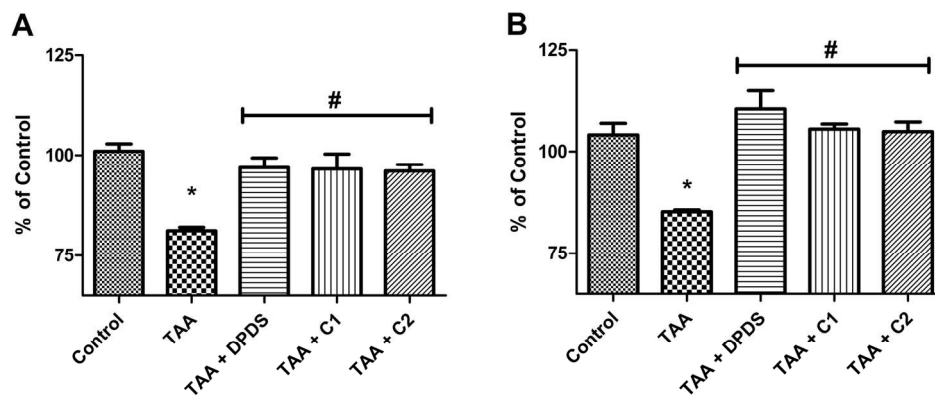
Fig 3
80x36mm (600 x 600 DPI)

Fig 4
81x36mm (600 x 600 DPI)

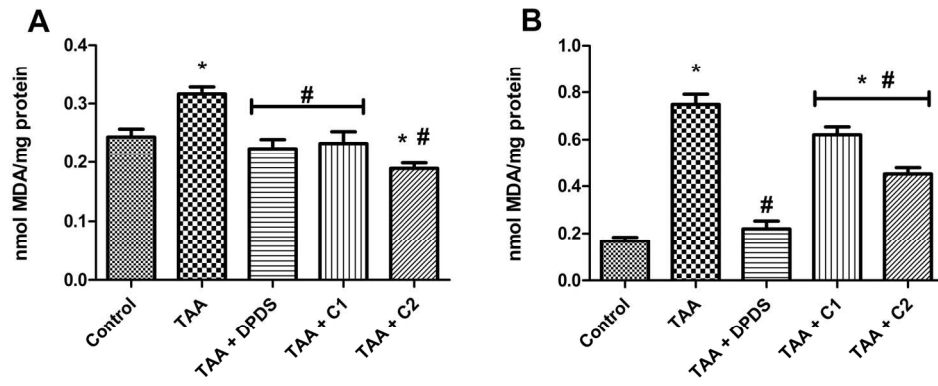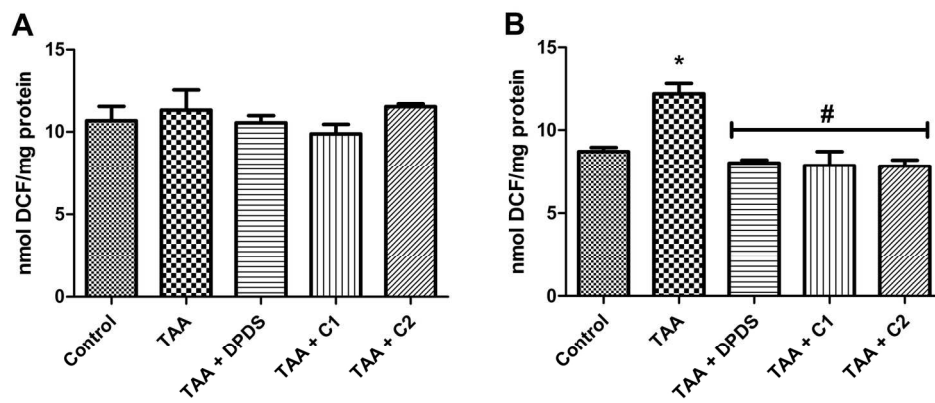Fig 5
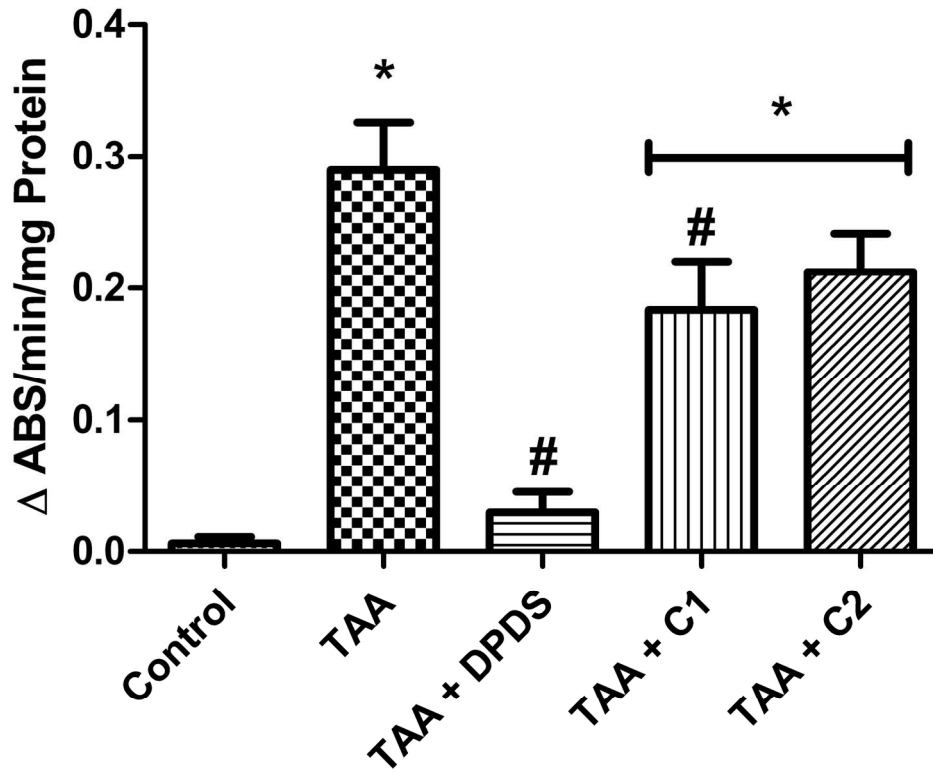79x34mm (600 x 600 DPI)

Fig 6
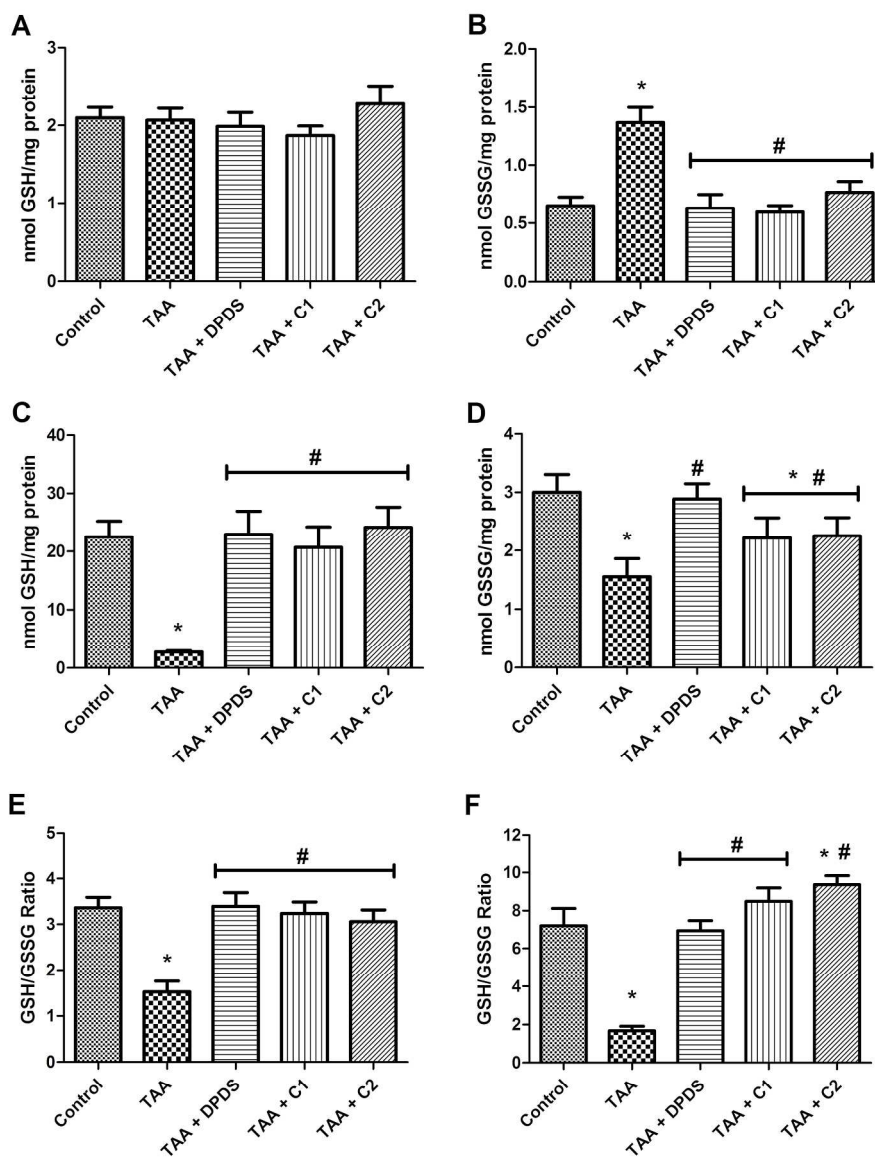82x36mm (600 x 600 DPI)
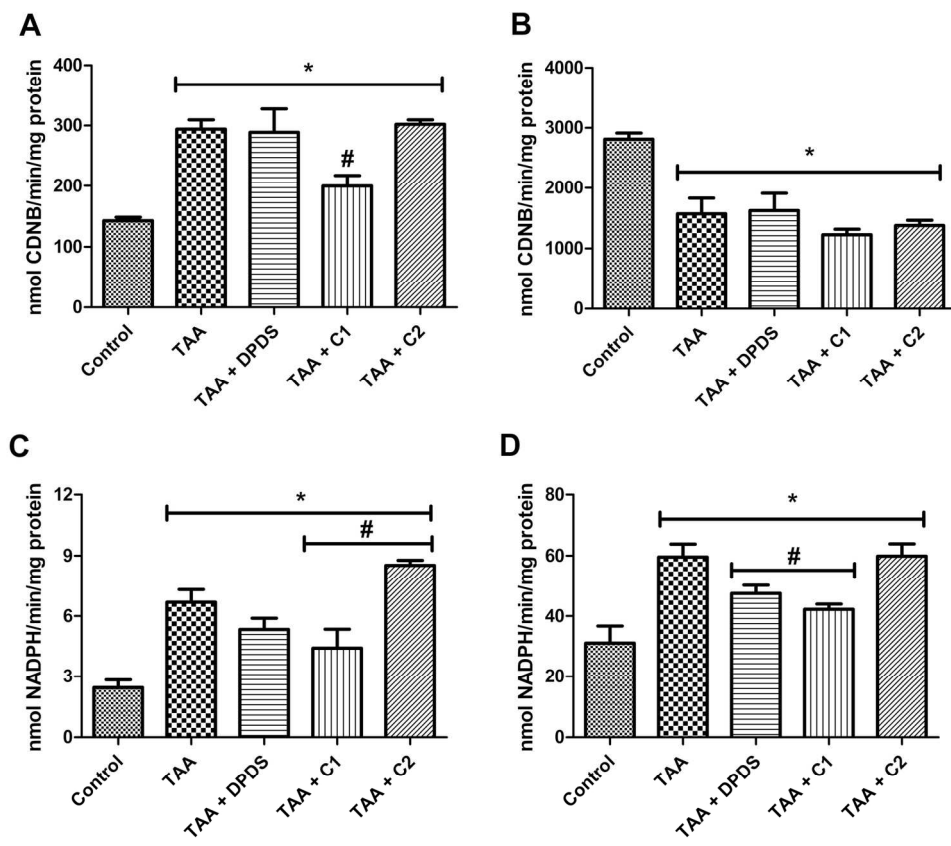
Fig 7
82x70mm (600 x 600 DPI)
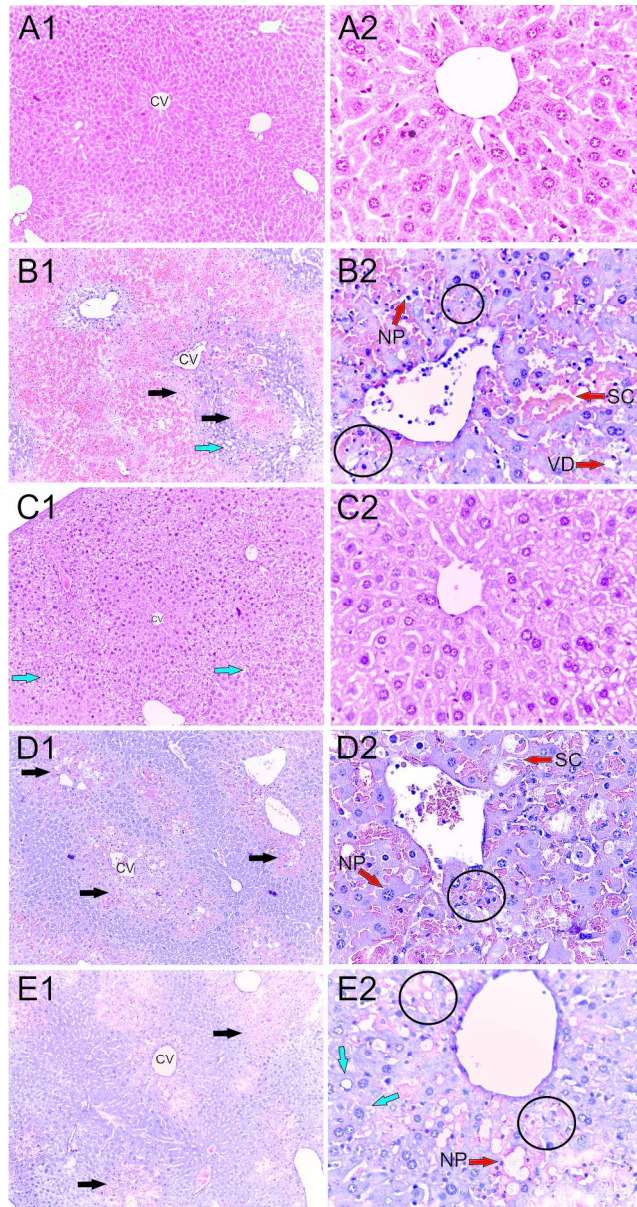
Fig 8
237x306mm (300 x 300 DPI)

Fig 9
163x144mm (300 x 300 DPI)

Fig 10
256x483mm (300 x 300 DPI)